Article

Applicability of Face Masks as Recyclable Raw Materials for Self-Made Insulation Panels

Eugenia Rossi di Schio [1], Vincenzo Ballerini [1], Jan Kašpar [2], Manuela Neri [3], Mariagrazia Pilotelli [3], Edoardo Alessio Piana [3] and Paolo Valdiserri [1,*]

1   Department of Industrial Engineering, Alma Mater Studiorum—University of Bologna, Viale Risorgimento 2, 40136 Bologna, Italy; eugenia.rossidischio@unibo.it (E.R.d.S.); vincenzo.ballerini2@unibo.it (V.B.)
2   Department of Chemical and Pharmaceutical Sciences, University of Trieste, Via L. Giorgieri 1, 34127 Trieste, Italy; kaspar@units.it
3   Department of Mechanical and Industrial Engineering, University of Brescia, Via Branze 38, 25123 Brescia, Italy; manuela.neri@unibs.it (M.N.); mariagrazia.pilotelli@unibs.it (M.P.); edoardo.piana@unibs.it (E.A.P.)
*   Correspondence: paolo.valdiserri@unibo.it

Abstract: The circular economy model is based on the 4R framework—reduce, reuse, recycle, and recover. While recycling was the primary focus in the past, the shortage of raw materials and the desire to reduce carbon footprints have led to a change in focus: end-of-life materials are now considered resources rather than waste. When discharged, end-of-life materials still possess properties that can be exploited. For this reason, a comprehensive characterization of reusable materials is mandatory to reduce waste and increase material availability. The reuse of waste materials, such as surgical masks, is of particular interest in giving people in disadvantaged contexts the opportunity to self-produce and self-install panels within their homes, with the dual result of improving indoor comfort and increasing human capital. This paper focuses on the identification of a possible second application for surgical face masks through experimental characterization. Panels made of masks were tested for water vapor permeability, thermal conductivity, and fire resistance and their use as insulating material in the building sector was discussed. Based on the results, surgical face masks are suitable as thermal insulating materials, do not pose safety concerns, and can reduce energy consumption and improve thermal comfort when installed indoors.

Keywords: surgical face masks; circular economy; sustainable materials; energy efficiency

1. Introduction

The United Nations calls for strategies aimed at environmental quality, economic prosperity, social equity, decent standards of living, and future generations [1]. As a reaction to the increasing energy costs, and pushed by the need to reduce carbon dioxide emissions, sustainability and the circular economy are now becoming integral parts of the building sector. In 2021, the operation of buildings accounted for 30% of global final energy consumption [2]. Despite several regulations and the availability of efficient and renewable energy sources, the decarbonization of the construction sector requires investments that not all realities can afford. The circular economy is based on business models able to replace the 'end-of-life' concept with the 4R framework—reduce, reuse, recycle, and recover [3]. Reusing aims at extending product life and reducing waste [4]. In contexts where material procurement is not feasible due to limited economic resources, reuse is a viable solution but, so far, it has been analyzed only partially. On the other hand, thermal insulating materials obtained by recycling waste are now very common, and they include materials derived from textiles [5,6], rubber [7], agriculture [7–9], cigarettes [10], and construction elements [11]. There has been an increase in the analysis of end-of-life materials (EoLHMs), such as plastic bottles [12], sponges [13], egg cartons [14], and clothes [15] as, when disposed

of, they still retain properties that can be exploited in other activities. Through local labor, EoLHMs could be converted into building elements for social inclusion.

One aspect that cannot be neglected is the possibility to support sustainable development, promoted by the United Nations through 1 of its 17 goals [1]. As part of this call, steps will be taken to reduce inequalities, improve health and education, and protect the environment. Moreover, Europe is facing the challenge of energy poverty in many contexts. As a result of their inability to pay the bills, people living in energy poverty are suffering from a lack of sufficient heating, cooling, and lighting. Symptoms of this situation include disease, death, and social isolation. Multidisciplinary approaches are necessary to eradicate this problem, considering technical, social, and policy factors. However, such interventions often require an initial budget that is only available to a limited number of people. The study presented in this paper seeks to shorten this gap by offering cost-effective solutions; to do this, building elements that can be obtained by residents of the dwellings to be improved were considered. Through the implementation of these solutions, residents can achieve decent living conditions.

An environmental threat was represented by the significant number of face masks used to face the COVID-19 pandemic. The use of masks is affected by demographic factors such as age, gender, urbanicity, and education levels, with more intensive use for older people, females, and those with higher education levels [16]. Due to the difficulty of separating face masks' basic materials and their contained size, in most municipal systems, face masks are not recyclable [17]: surgical masks along with plastic gloves in coastal regions are emerging sources of microplastic particles and secondary microfibers in marine environments [18] and urban rivers [19].

The littering of masks has presented a big problem, with consequent plastic debris ending up in urban rivers [19] and, consequently, in oceans, where the biodegradation process can take hundreds of years, resulting in pollution by micro- and nano-plastic particles [20]. Several other solutions have been proposed, including biodegradable, disposable masks; mask-only trash cans; guidelines; and strict waste management. From the perspective of reuse, a possible disinfection method was investigated in [21]. This method was based on a sustainable and fast vacuum ultraviolet (VUV) treatment for the disinfection of N95 masks that had no structural damage and functional decline and were up to the reuse standard. Reusing masks outside surgical settings offers notable benefits in waste management while maintaining the safety of the individuals who use them, whether in the general population, industries, or hospitals [22]. Moreover, Alcaraz et al. [22] examined the feasibility of cleaning medical masks to ensure their safety and functionality for reuse, exploring the environmental advantages associated with managing medical disposable waste, despite the current designation of masks as single-use by regulatory frameworks. Indeed, IIR, namely, medical face masks classified as Type II according to bacterial filtration efficiency and splash resistance, are polypropylene medical masks that can be washed up to 10 times, washed 5 times and autoclaved 5 times, or washed and then sterilized with radiation or ethylene oxide, without any degradation of their filtration or breathability properties, although there is loss of the anti-projection properties. In detail, the breathability and filtration efficiency of face masks after washing and decontamination processes were investigated in [23]. Other studies focused on reusing bulk residuals from the face mask production process to realize panels with thermal and acoustic properties [24] and for cement production [25–27]. In [25], shredded and cut single-use face masks were added as fiber in a mortar that enhanced flexural strength and mitigated shrinkage, carbonation degree, and water absorption. Both scenarios withstand crack propagation and offer gradual failure.

In [26], Kilmartin-Lynch et al. proposed the reuse of face masks to improve the quality of concrete. The authors cut up single-use masks by first removing the ear loops and inner nose wire to size and spread them throughout five different mix designs to explore possible benefits and uses within concrete in percentages of 0.10%, 0.15%, 0.20%, and 0.25% by concentrating on compressive strength, indirect tensile strength, modulus of elasticity, and ultrasonic pulse velocity to test the overall quality of the concrete. The inclusion of

single-use face masks resulted in an increase in the strength properties of the concrete samples, as well as an increase in the overall quality of the concrete. However, beyond 0.20%, the trend of increasing strength decreased.

The analysis presented by Koniorczyk et al. [27] instead focused on processed face masks that were converted into fiber to be added to mortar. The results obtained indicated that the addition of processed masks slightly increased the compressive strength (by about 5%) and decreased the tensile strength (by about 3%). It was also reported that the addition of the masks did not affect material properties related to concrete durability such as frost resistance, water permeability, and fire performance. Experiments were performed on bound composite materials using the discarded face masks and wood adhesive as a binder. Initially, the discarded face masks underwent a heating process lasting one and a half hours at 120 °C to eliminate any potential contaminants, be they biological or otherwise. Subsequently, five different composites were created: the first incorporated the complete face masks, the second used face masks with iron nose clips only, the third used face masks lacking both ear loops and iron nose clips, the fourth contained the elastic ear loops exclusively, and the fifth had face masks with only elastic ear loops [28]. The polymerized binder percentage significantly affected the thermal conductivity coefficient.

In the present study, surgical face masks (hereafter referred to as SFMs) were analyzed experimentally to propose self-realizable panels to be installed indoors to reduce the energy demand in the heating season and improve thermal comfort in disadvantaged contexts (such as social housing). SFMs' structure, water vapor permeability, thermal conductivity, and fire resistance were investigated experimentally and the effect of their arrangement, dimension, and density was analyzed along with the effect of sanitation and fire retardant treatments. As far as the authors are concerned, this experimental characterization has never been performed in the literature. Water vapor permeability and thermal conductivity measurement tests were performed at the Laboratory of Thermal Engineering and Industrial Energy Systems at the University of Bologna and the Ecam Ricert in Vicenza (Italy). Tests to assess fire resistance were performed at the Department of Chemical and Pharmaceutical Sciences at the University of Trieste (Italy).

2. Materials and Methods

Experimental and numerical analyses were performed to assess the suitability of SFMs for applications in the construction sector and building energy refurbishment. The SFMs analyzed (Figure 1) were made of 67% non-woven fabric and 33% melt-blown fabric for a total of three layers: the outmost layer was made of polypropylene spun-bonded non-woven fabric and had waterproof and bacteriostatic properties, the filtrating intermediate layer was made of PP melt-blown superfine fiber, and the innermost layer was made of non-woven fabric with water-absorbing and skin-friendly properties [29]. A metal insert in the top part (white strip in Figure 1) facilitated positioning on the nose.

Both untreated and treated SFMs were considered. The first treatment considered was sanitization. A subset of the sanitized masks also received an additional fire retardant treatment. The sanitization process consisted of a 60 °C dishwasher cycle for a duration of 60 min followed by a one-week drying process in ambient air. This was consistent with the observation that a significant degree of inactivation of pathogenic species occurs at 60 °C, and several virus types, e.g., COVID-19, are among those highly sensitive to thermal degradation [30,31]. The wet impregnation of the fire retardant was performed using a commercial flame retardant (FEUERFEST®Fire protection impregnation for textiles, DIN 4102). SMFs were soaked for 5 min in the fire retardant liquid, then drained and dried for 3 days. SFM loading of 8 wt% was attained.

2.1. Experimental Activities

The analyzed SFM properties were morphology, water vapor resistance, fire resistance, and thermal conductivity.
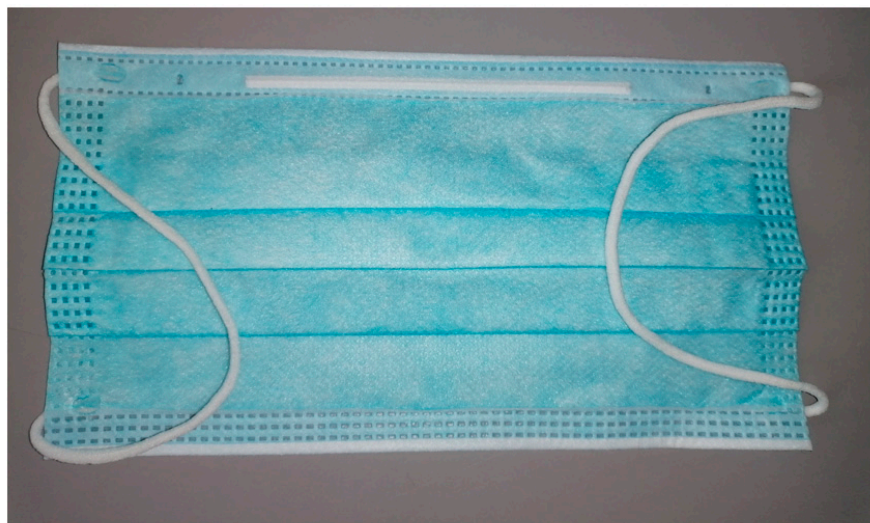
Figure 1. Surgical face masks analyzed in this study.

2.1.1. Sample Morphology Detected by Optical Microscopy

SFM samples were analyzed using an optical microscope equipped with a Dino-lite AM4023 digital eyepiece camera with a 1.3 Megapixel resolution. The morphology of the face masks was compared to that of two widely employed insulating materials, i.e., polystyrene and rock wool. The images are shown in Figure 2. The observed patterns appeared well in line with the origin of the materials: polystyrene showed typical features of an irregular foam-type surface with diffuse porosity (pore diameter ≤ 85 μm) (Figure 2C), whereas both rock wool and SFM featured typical aspects of a fibrous type of insulation material, with a ratio length/diameter well over 10. The diameter of the fibers in the rock wool appeared slightly thinner compared to the SFM layer of PP melt-blown superfine fibers and, more importantly, the web of the rock wool fibers featured a higher density of fibers compared to SFM. A perusal of the SFM micrograph revealed that there was a soft compact layer under the fibrous level consistent with the multilayer structure of the SFM.

2.1.2. Fire Resistance Analysis

The fire resistance of the SFMs, both untreated and fire retardant-treated, was tested using the Temperature Programmed Oxidation technique [32]. This technique, which consisted of heating a sample of the SFM in a flow reactor using a constant heating rate of 10 °C/min from room temperature up to 500 °C with a flow of air (200 mL/min), allowed us to directly detect the auto-ignition temperature of the material, i.e., the temperature at which the material spontaneously combusted. In a typical experiment, a rectangular piece (ca. 10–15 × 2–3 mm, 7–15 mg) was cut out from the central part of the SFM, loaded into a U-shaped flow microreactor (Figure 3), and then subjected to the above quoted thermal treatment. The reactor out-flow was continuously analyzed using a Multigas 2030 FTIR analyzer made by MKS instrument Inc., Andover (MA), USA.

An inspection of Figure 4 reveals similar features for both untreated and fire retardant-treated samples; both samples ignited at about 200 °C, although there was some change in the combustion pattern, as denoted by CO_2 evolution: the broad peak with a maximum at about 400 °C in the untreated sample was split into two overlapping peaks at 295 °C and 415 °C. The molar compositions of the emitted gases were not significantly affected, 65% vs. 65 % for CO_2, 20% vs. 24% for CO, 3% vs. 3% for CH_4 12% and 12% vs. 13% for acetaldehyde, respectively, in the untreated and retardant-treated SFMs. Conversely, the total amount of evolved gases in the retardant-treated SFM decreased by 20% mol with respect to the untreated one. Consistently, some solid uncharacterized deposit was found in a cold zone at the outlet of the TPO reactor.
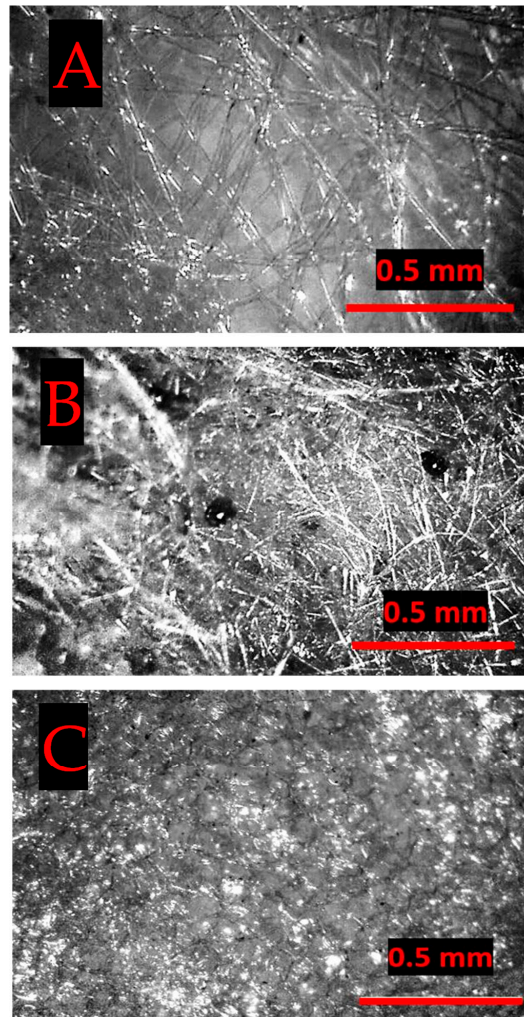
Figure 2. Micrographs of surgical face mask (**A**), rock wool (**B**), and polystyrene (**C**).
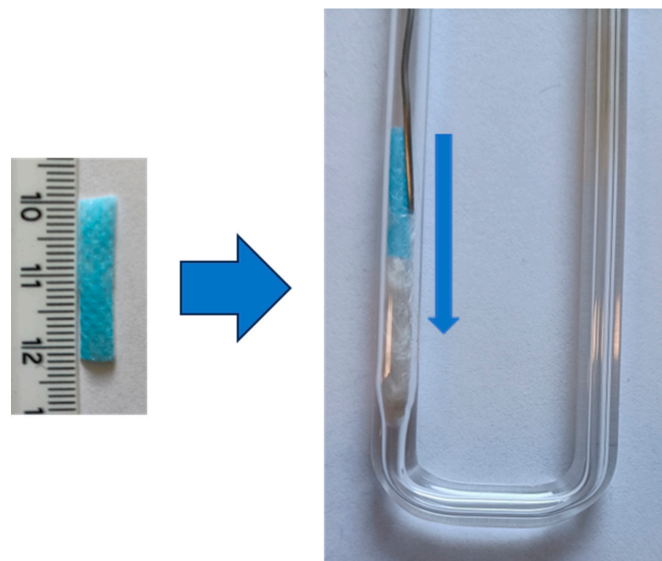

Figure 3. Test specimen made for the fire resistance analysis (SFM sample) and the flow microreactor loaded with the SFM (right arrow): The vertical arrow indicates the direction of the airflow. A K-thermocouple was vertically inserted into the SFM layer to continuously monitor the temperature. The SFM was held in place using glass wool.
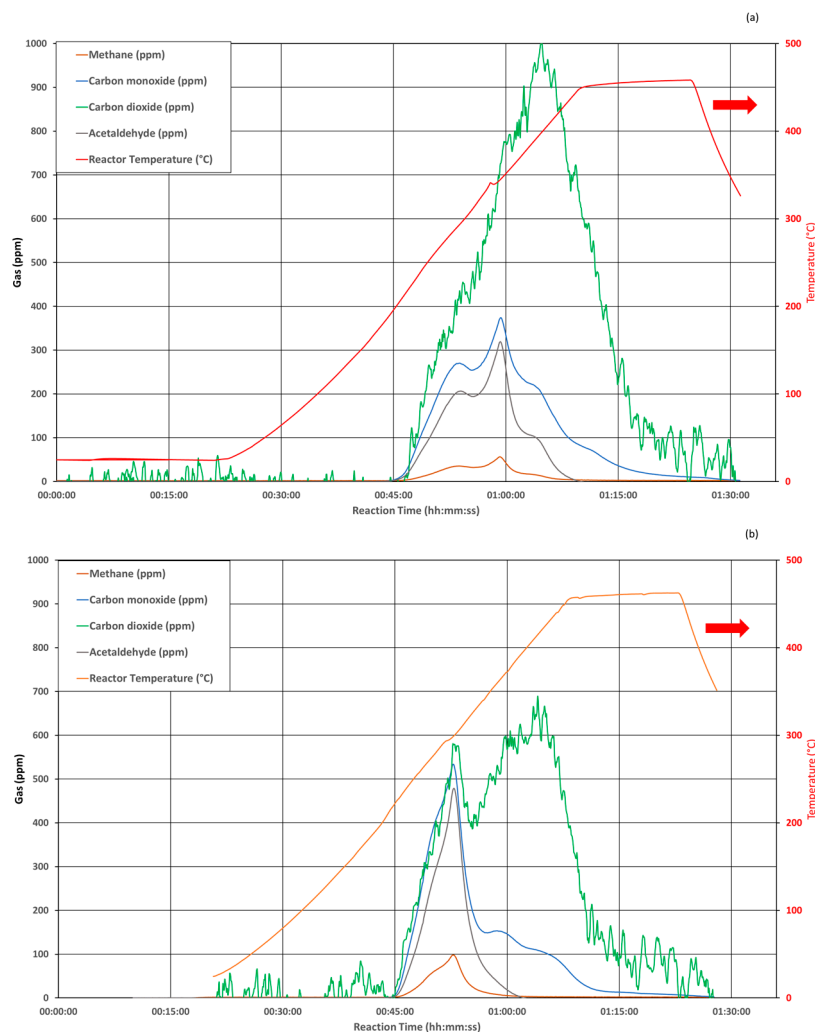
Figure 4. Examples of Temperature Programmed Oxidation profiles obtained on (**a**) untreated and (**b**) fire retardant-treated SFMs. Gas concentration (ppm) and temperature profile (°C) are reported as a function of time (hh:mm:ss).

2.1.3. Water Permeability

The water vapor transmission rate of a sample made by stacking 20 SFMs for a total of 6.3 cm in thickness was evaluated through a water vapor permeability test carried out in accordance with the EN 12086 [33] standard. As shown in Figure 5, the sample was placed at the top of a holder element while, at the bottom, there was a desiccant-saturated solution of water and potassium nitrate KNO_3.

The sample was placed in a chamber with controlled humidity and temperature. At regular time intervals, the sample was weighed using a precision weighing scale to determine the total mass of the vapor passed through the mask layer (Figure 6). The test was performed in a condition defined as 'A', which required a pressure difference of 1400 Pa for the determination of the water vapor permeability. The resulting water vapor permeability δ was about 176×10^{-12} kg/(m s Pa).
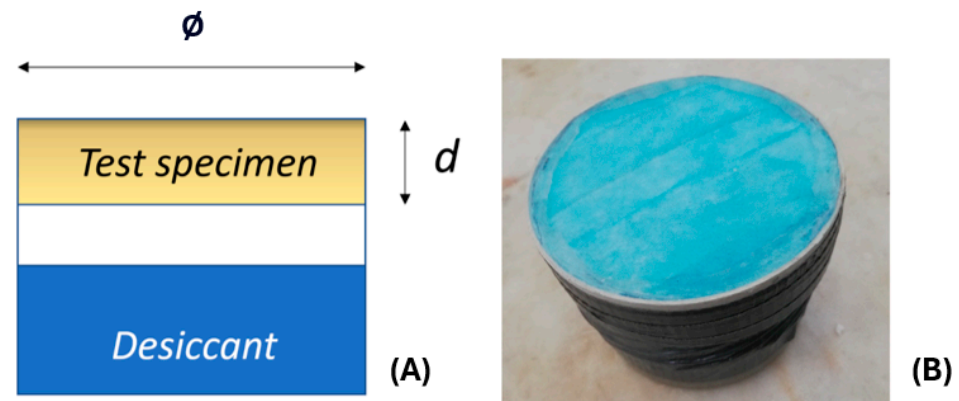
Figure 5. Section of the test specimen made for the water vapor (**A**) test and picture of the sample (**B**). The sample diameter (Ø) was 9 cm, while the sample thickness *d* was 6.3 cm. A total of 20 face masks were used.
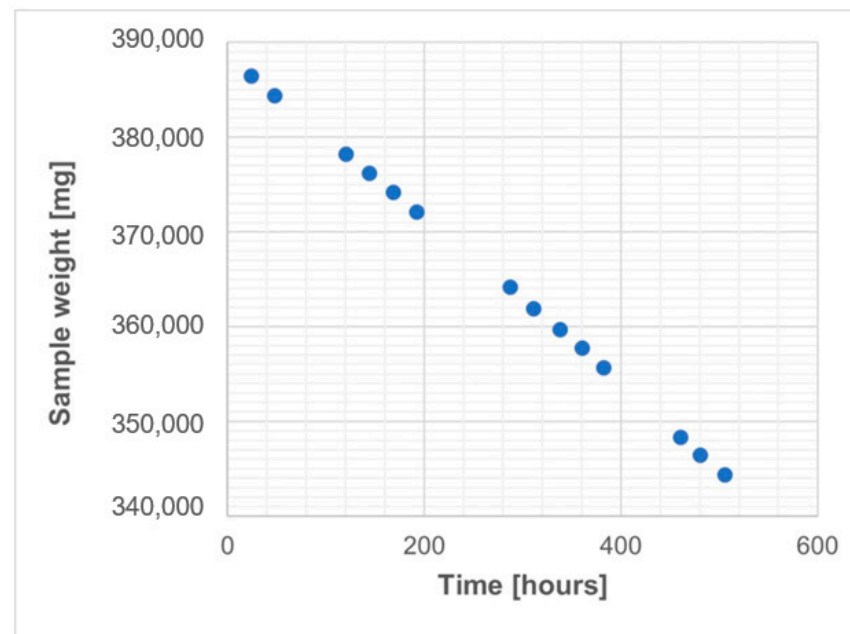

Figure 6. Sample weight along the water vapor permeability test.

2.1.4. Thermal Conductivity

The analyzed sample, shown in Figure 7, was made of a cardboard frame measuring 0.5 m × 0.5 m × 0.08 m in which SFMs were placed in different manners. The masks were weighed, folded (if necessary), and stacked in the frame to achieve the desired density. Finally, the SFMs were compacted by closing the shell.

Thermal conductivity tests were conducted at the University of Bologna (Italy) and the Ecam Ricert Institute of Monte di Malo—Vicenza (Italy). The first case involved a heat flow meter designed to analyze material with a thermal conductivity of less than 5 W/(m K), following the ISO 8301 [34] standard. The test apparatus used in the second laboratory was a commercial guarded hot plate (model Lambda Meter EP500) manufactured by Lambda Messtechnik GmbH Dresden (Dresden, Germany), in accordance with the EN 1946-2 [35] standard. In the test, the sample was placed between a hot and a cold plate kept at constant temperatures by two thermostatic baths, and an insulating layer reduced lateral heat losses. Data were acquired by means of a multimeter, a switch control unit, and an ice point reference.
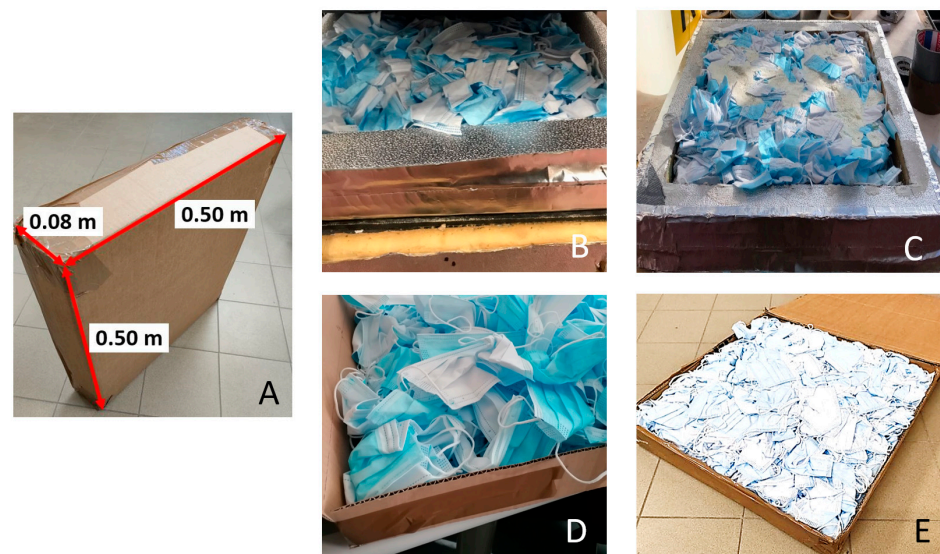
Figure 7. Test specimens made for the thermal conductivity tests: dimensions of the specimens (**A**), shredded masks (**B**), shredded masks with polyurethane foam (**C**), and two phases of the panel realization with crumpled masks (**D,E**).

Several aspects were analyzed, such as panel density, operator manual skills, the presence of metallic elements and foams, and the effect of some treatments. Panel density ranged between 30 and 90 kg/m^3 (corresponding to a number of masks in the panel of about 200 and 600, respectively, considering the unit weight of a mask to be 0.003 kg), which are typical values for commercial insulating materials. In view of panel self-realization, SFMs were crumpled and/or shredded to assess the influence on operator manual skills. The effect of polyurethane foam and metal elements in the panel was also analyzed.

Tests performed on untreated SFMs—non-sanitized and without fire retardants—are summarized in Table 1. SFM arrangement and density are identified by an acronym: the letters refer to the masks' arrangement—ordered (O), casual arrangement (D), crumpled (C), and shredded (S)—while the number refers to the panel density (in kg/m^3). For the ordered, disordered, and crumpled arrangements, the masks were left intact, while, for the shredded arrangement, they were cut to facilitate their packing. To assess how the thermal conductivity was affected by the assembling phase, for the samples filled with crumpled masks, two repetitions were performed for some tests (denoted with the number 2) in which the masks were casually rearranged. Tests where the metallic nose clip was removed are identified with the letter W. Finally, two tests (S_54_W and S_63_W) were performed by adding a polyurethane foam both superficially and laterally through a nozzle. The results are reported in Table 1 and displayed in Figure 8.

Since end-of-life SFMs cannot be used directly after being used by people and need to undergo a fire retardant process, the effect of two treatments was analyzed. The sanitization was carried out through a washing machine process, while the fire retardant process consisted of the application of a flame retardant designed for textiles. Table 2 summarizes the tests performed, while the results are displayed in Figure 9, where they are compared to the reference case T1 performed on untreated SFMs.

Table 1. Tests performed on non-sanitized masks to determine the panels' thermal conductivity.

| Test Name	Sample Characteristics	ρ (kg/m^3)	λ_{eq} (W/mK)
O_60	Masks in an ordered arrangement	60	0.046
O_90	Masks in an ordered arrangement	90	0.039
D_90	Masks in a disordered arrangement	90	0.042
C_30_1	Crumpled masks	30	0.072
C_30_2	Crumpled masks—repetition	30	0.064
C_40_1	Crumpled masks	40	0.055
C_40_2	Crumpled masks—repetition	40	0.047
C_50_1	Crumpled masks	50	0.051
C_50_2	Crumpled masks—repetition	50	0.059
C_60_1	Crumpled masks	60	0.047
C_60_2	Crumpled masks—repetition	60	0.052
C_70_1_W	Crumpled masks without clip-on	70	0.045
C_70_2_W	Crumpled masks without clip-on	70	0.047
C_76_1	Crumpled masks	76	0.052
C_76_2	Crumpled masks—repetition	76	0.052
S_30	Shredded masks without clip-on	30	0.052
S_50	Shredded masks without clip-on	50	0.043
S_54_W	0.355 kg of shredded masks in polyurethane foam (44%) without clip-on	54	0.048
S_63_W	0.59 kg of shredded masks in polyurethane foam (21%) without clip-on	63	0.041
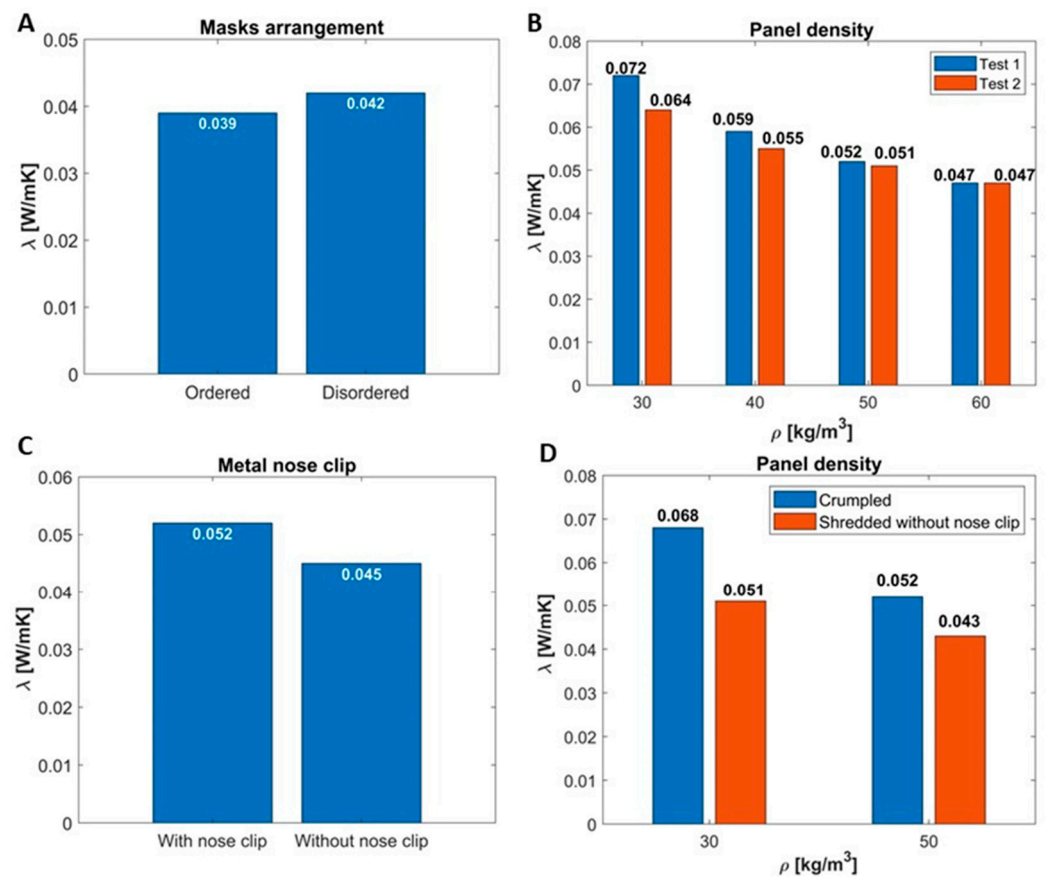
Figure 8. Thermal conductivity as a function of the mask arrangement (ϱ = 90 kg/m^3) (**A**), density and arrangement (the second test was performed by casually reshuffling the masks) (**B**), presence of the nose clip-on (**C**), SFM dimensions (**D**).

Table 2. Tests performed on SFMs sanitized and treated with flame retardant. Crumpled masks were used to realize the panel. Each test is identified by an acronym: "Sa" indicates sanitized; "SFR" sanitized and fire retardant treatment. The final number is the panel density. The uncertainty of the measurement is ±0.001.

Test Name	Sanitized	Flame Retardant	ρ (kg/m^3)	λ_{eq} (W/(mK))
T1			75	0.053
Sa_60	✔		60	0.066
Sa_70	✔		70	0.060
Sa_75	✔		75	0.059
Sa_80	✔		80	0.054
Sa_90	✔		90	0.050
SFR_60	✔	✔	60	0.053
SFR_64	✔	✔	64	0.052
SFR_70	✔	✔	70	0.050
SFR_75	✔	✔	75	0.059
SFR_80	✔	✔	80	0.044
SFR_83	✔	✔	83	0.043
SFR_90	✔	✔	90	0.052

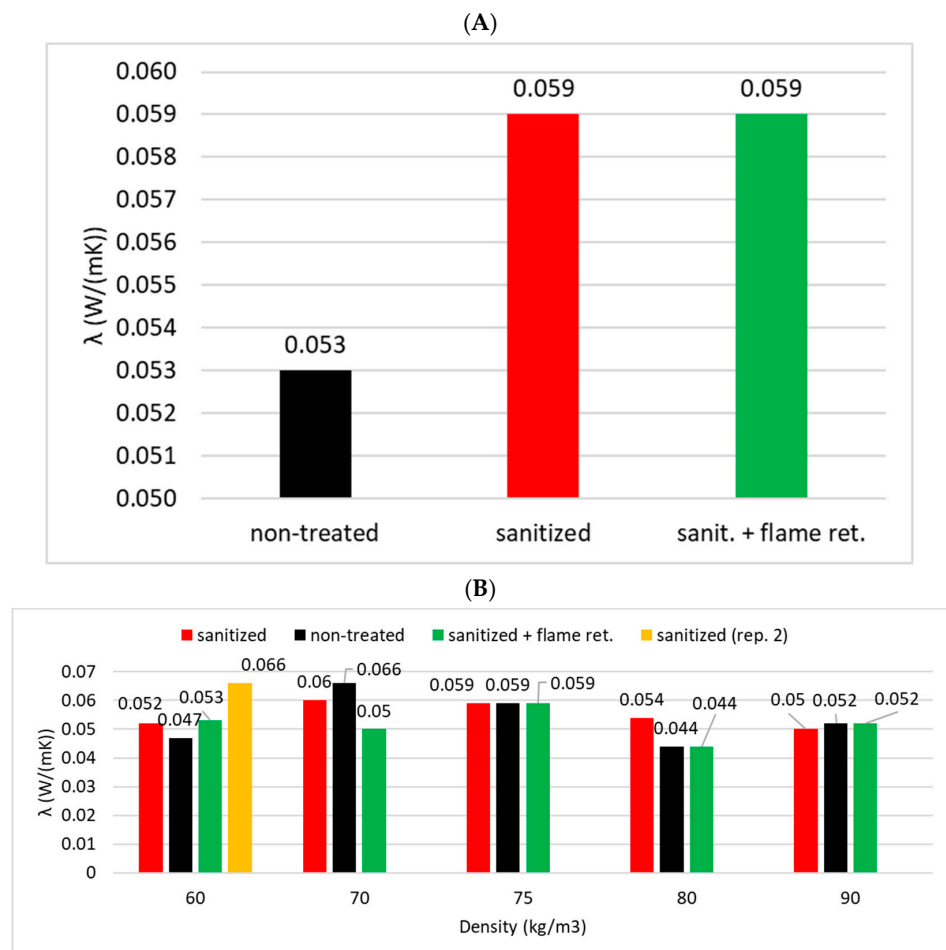**(A)**

(B)

Figure 9. Thermal conductivity as a function of the treatment (density 75 kg/m^3 made with crumpled masks) (**A**) and the density (**B**). Values were measured for panels made with non-treated, sanitized (where "sanitized (rep. 2)" is the second test repetition conducted at the same density), and impregnated with flame retardant (sanit. + flame ret.) masks.

3. Discussion

The experimental and numerical results are here discussed to determine whether SFMs are suitable for the realization of panels to be installed indoors to improve comfort and reduce energy demands during the heating season.

3.1. SFM Characterization and Fire-Resistance of SFMs

The microscope analysis (Figure 2) clearly revealed that the morphology of the SFMs represented similar features to fibrous types of insulating materials such as rock wool, with comparable thickness and length of the fibers; yet, the density of the fibrous web appeared less dense than that of the rock wool. Consequently, thermal conductivity comparable to that of fibrous materials was expected. Moreover, compaction or any treatment affecting the space distribution of the web of fibrous elements could in principle affect thermal behavior.

As far as the fire resistance of SFMs is concerned, it must be recalled that PP ignition temperature is reported in the literature to be 570 °C [36]; yet, this value is related to massive, extruded PP. Our results appear to be very consistent with those reported in [37], where it was observed that the combustion of SFMs started at about 200 °C in thermogravimetric measurements carried out in air. Large PP particles showed lower reactivity compared to fine ones, indicating that the larger the exposed surface, the higher the reactivity [38]. Figure 2 shows a fibrous structure of a PP layer with a typical fiber diameter of 3.2×10^{-4} cm. Assuming an average length of the fibers of 1 cm, a surface area of 1.39×10^4 cm^2/g was calculated for the fiber, which would drop to 6.67 cm^2/g for a single cubic piece. Such an order of magnitude variation of the surface area is clearly expected to change the reactivity of the material.

The observation that the starting temperature of the combustion was slightly affected by the fire retardant can be attributed to the mechanism of the fire retardancy effect [36], which, in our case, was related to an endothermic effect, as checked by separate experiments (data not reported). These experiments were carried out using glass wool impregnated with a pure fire retardant, which showed a neat endothermic phenomenon that started at around 200 °C, i.e., the temperature at which the samples ignited. Consistently, we found some increase in CO production in the treated sample, indicating a slightly higher extension of the partial combustion and fewer gases evolving compared to the untreated sample. With both ignition and endothermic phenomena occurring at the same temperature, significant fire retardancy was not expected. There are several studies reporting the effects of fire retardants on the combustion behavior of PP, all indicating that, due to the high flammability of PP, the use of a combination of fire retardants is necessary to achieve significant protection (see, for example, [39]); moreover, endothermal effect-based fire retardants generally require the use of high loading, which was not applicable in our case. Other results clearly explain our observations; although, we must keep in mind that for the targets of this research, only simple, cheap, and easy-to-apply solutions must be employed for panel production.

3.2. Vapor Permeability and Thermal Conductivity

The measured water vapor permeability, equal to 1.76×10^{-10} kg/(m s Pa), was comparable to that of other fibrous insulating materials, such as mineral wools and glass wool (that are in the order of 1.50×10^{-10} kg/(m s Pa)).

With regard to thermal conductivity, several aspects were analyzed. As a general comment, the thermal conductivity values here reported for the panels were in the typical range of items made with fibrous materials, consistent with the SFM microstructure depicted in the micrographs (Figure 2): 0.044 and 0.037 W/m K thermal conductivity was reported respectively for rock wool and polystyrene [39]. Data in Figure 8A obtained on non-sanitized masks show that the masks' arrangement in the panel affected the thermal conductivity, which ranged between 0.039 W/mK for ordered masks and 0.042 W/mK for disordered masks. The random shuffling of masks meant that the panel was not uniformly filled, allowing air to circulate and increasing the heat transfer; this aspect was also confirmed by the results in Figure 8B, determined by repeating the tests for the same panel

density but shuffling the masks: two different thermal conductivity values were obtained for the same panel density. Thermal conductivity was a decreasing function of density, but the masks' positioning was less important for higher density values. This was due to the minor quantity of voids left when masks were tidily stacked. The metallic nose clip affected thermal performance (Figure 8C): when the metal element was removed, the thermal conductivity was reduced from 0.052 to 0.045 W/mK. Cutting the masks resulted in an improvement in thermal performance, as can be seen in Figure 8D, where, in this case, it was also a decreasing function of density. Ideally, the metal element should be removed and the masks should be cut into smaller pieces, but, since both operations are time-consuming, a cost/benefit assessment would be necessary, especially if implemented on a medium/large scale. According to Figure 9, SFM treatment determined an increase in thermal conductivity. However, a clear pattern between sanitized and flame retardant treatment was not evident (Figure 9A), even if it seemed that lower values were detected with higher density. For sanitized masks, the thermal conductivity decreased with density (as seen for the untreated templates), but, for the flame retardant-treated masks, there was no discernible trend since the highest conductivity value was found for the panel with a density of 75 kg/m^3. This may have been due to uneven product application.

3.3. Comparison with Properties of Materials in the Literature

The thermal conductivity measured for the panels made with SFMs was compared with that given for other EoLHMs reported in the literature. Figure 10 compares the thermal performance of SFMs with those of bulk polyamide, a waste material from the production of non-surgical face masks. The bulk material showed lower thermal conductivity, and this was due to the structure of SFMs, which did not allow for voids to be completely filled in the panel, and the presence of the metal nose clip. On the other hand, the thermal conductivity of panels made with SFMs was lower than that of panels made using EoLHMs such as egg boxes, polyester, and felt.
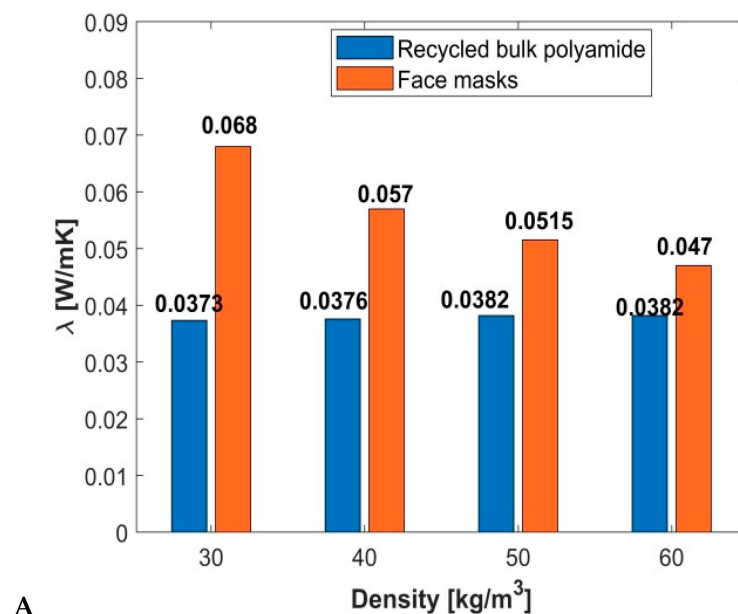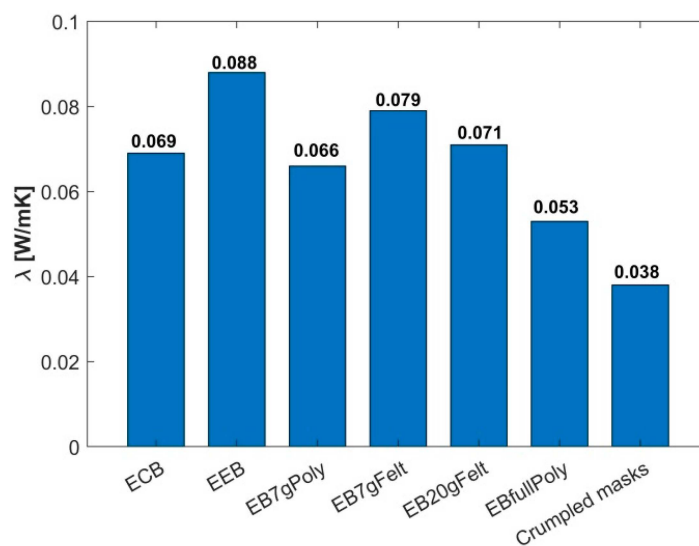

Figure 10. *Cont.*

B

Figure 10. Comparison of the thermal conductivity measured for panels made with recycled polyamide-66 [40] and crumpled face masks (**A**). In (**B**), the comparison of the thermal conductivity measured for panels made with a cardboard box filled with crumpled masks (Crumpled masks) is reported with that measured for panels made of cardboard boxes filled with different materials and presented in [15]. In this latter case, ECB refers to an empty cardboard box 7 cm thick (with air in the box); in EEB, the cardboard box contained egg boxes, and each egg box was filled with 7 g of polyester in EB7gPoly, 7 g felt in EB7gFelt, and 20 g felt in EB20gFelt. The cardboard box was filled with polyester in EBfullyPoly (but no egg boxes).

4. Conclusions

This study explored new ways to foster the circular economy model and encourage the reuse of EoLHMs for applications in the building sector. The focus was on the properties of surgical face masks, and attention was paid to complete face masks, face masks with only iron nose clips, face masks (no loops and iron nose clips), face masks with elastic loops only and a high binder ratio (no iron nose clip), and face masks with elastic loops only but a low binder ratio.

The experimental results show that SFMs' water vapor permeability is comparable to that of other porous materials such as mineral and glass wool. The measured thermal conductivity ranged from 0.039 to 0.072 W/(m K), which is typical of items made with fibrous materials.

However, the thermal conductivity depends on the masks' arrangement, dimensions, and density. Thermal conductivity was affected by sanitization and flame retardant treatment, with higher values for treated masks, but no recognizable pattern was observed. As density increased, thermal conductivity decreased. There was an important influence from the nose clip-on since, when it was removed, the thermal conductivity was reduced. Placing masks neatly and removing the metal element was the best method for making panels, but this method would generate board construction difficulties in large-scale production. The addition of polyurethane foam seems not to be beneficial. The observed ignition temperature and the minimal effect of the flame retardant suggest that the use of an insulating panel with a gypsum board embedded for fire protection is required.

In this paper, the authors reported results that may lead to new ways to use EoLHMs. Attention was paid to surgical face masks, and future analyses will consider other possible materials.

Data Availability Statement: The data presented in this study are available on request from the corresponding author.

Conflicts of Interest: The authors declare no conflicts of interest.

References

1. United Nations, Department of Economic and Social Affairs, Sustainable Development. The 17 Goals. Available online: https://sdgs.un.org/goals (accessed on 6 November 2023).
2. IEA. *Buildings*; IEA: Paris, France, 2022; Available online: https://www.iea.org/reports/buildings (accessed on 6 November 2023).
3. Kirchherr, J.; Reike, D.; Hekkert, M. Conceptualizing the circular economy: An analysis of 114 definitions. *Resour. Conserv. Recycl.* **2017**, *127*, 221–232. [CrossRef]
4. Neri, M.; Pilotelli, M.; Traversi, M.; Levi, E.; Piana, E.A.; Bannó, M.; Cuerva, E.; Pujadas, P.; Guardo, A. Conversion of end-of-life household materials into building insulating low-cost solutions for the development of vulnerable contexts: Review and outlook towards a circular and sustainable economy. *Sustainability* **2021**, *13*, 4397. [CrossRef]
5. Dissanayake, D.G.K.; Weerasinghe, D.U.; Thebuwanage, L.M.; Bandara, U.A.A.N. An environmentally friendly sound insulation material from post-industrial textile waste and natural rubber. *J. Build. Eng.* **2021**, *33*, 101606. [CrossRef]
6. Hadded, A.; Benltoufa, S.; Fayala, F.; Jemni, A. Thermo physical characterisation of recycled textile materials used for building insulating. *J. Build. Eng.* **2016**, *5*, 34–40. [CrossRef]
7. Wang, J.; Du, B. Experimental studies of thermal and acoustic properties of recycled aggregate crumb rubber concrete. *J. Build. Eng.* **2020**, *32*, 101836. [CrossRef]
8. Limami, H.; Manssouri, I.; Cherkaoui, K.; Khaldoun, A. Physicochemical, mechanical and thermal performance of lightweight bricks with recycled date pits waste additives. *J. Build. Eng.* **2021**, *34*, 101867. [CrossRef]
9. Othmani, C.; Taktak, M.; Zein, A.; Hentati, T.; Elnady, T.; Fakhfakh, T.; Haddar, M. Experimental and theoretical investigation of the acoustic performance of sugarcane wastes based material. *Appl. Acoust.* **2016**, *109*, 90–96. [CrossRef]
10. Gómez Escobar, V.; Maderuelo-Sanz, R. Acoustical performance of samples prepared with cigarette butts. *Appl. Acoust.* **2017**, *125*, 166–172. [CrossRef]
11. Gruhler, K.; Schiller, G. Grey energy impact of building material recycling—A new assessment method based on process chains. *RCR Adv.* **2023**, *18*, 200139. [CrossRef]
12. Taaffe, J.; O'Sullivan, S.; Rahman, M.E.; Pakrashi, V. Experimental characterisation of Polyethylene Terephthalate (PET) bottle Eco-bricks. *Mater. Des.* **2014**, *60*, 50–56. [CrossRef]
13. Kang, C.W.; Kim, M.; Jang, E.S.; Lee, Y.H.; Jang, S.S. Sound absorption coefficient and sound transmission loss of porous sponge attached corrugated cardboard of noise insulation cover. *Palpu Chongi Gisul/J. Korea Tech. Assoc. Pulp Pap. Ind.* **2020**, *52*, 38–44. [CrossRef]
14. Algaily, B.; Puttajukr, S.; Navarat, T. Acoustic absorption, rheological and mechanical characteristics of waste egg boxes fibers filled SBR. *J. Teknol.* **2015**, *77*, 45–52. [CrossRef]
15. Neri, M. Thermal and Acoustic Characterization of Innovative and Unconventional Panels Made of Reused Materials. *Atmosphere* **2022**, *13*, 1825. [CrossRef]
16. Badillo-Goicoechea, E.; Chang, T.H.; Kim, E.; LaRocca, S.; Morris, K.; Deng, X.; Chiu, S.; Bradford, A.; Garcia, A.; Kern, C.; et al. Global trends and predictors of face mask usage during the COVID-19 pandemic. *BMC Public Health* **2021**, *21*, 2099. [CrossRef] [PubMed]
17. Ibn-Mohammed, T.; Mustapha, K.B.; Godsell, J.; Adamu, Z.; Babatunde, K.A.; Akintade, D.D.; Acquaye, A.; Fujii, H.; Ndiaye, M.M.; Yamoah, F.A.; et al. A critical analysis of the impacts of COVID-19 on the global economy and ecosystems and opportunities for circular economy strategies. *Resour. Conserv. Recycl.* **2021**, *164*, 105169. [CrossRef] [PubMed]
18. Akhbarizadeh, R.; Dobaradaran, S.; Nabipour, I.; Tangestani, M.; Abedi, D.; Javanfekr, F.; Jeddi, F.; Zendehboodi, A. Abandoned COVID-19 personal protective equipment along the Bushehr shores, the Persian Gulf: An emerging source of secondary microplastics in coastlines. *Mar. Pollut. Bull.* **2021**, *168*, 112386. [CrossRef]
19. Wang, F.; Wu, H.; Li, J.; Liu, J.; Xu, Q.; An, L. Microfiber released into urban rivers from face masks during COVID-19. *J. Environ. Manag.* **2022**, *319*, 115741. [CrossRef]

20. Tabatabaei, M.; Hosseinzadeh-Bandbafha, H.; Yang, Y.; Aghbashlo, M.; Lam, S.S.; Montgomery, H.; Peng, W. Exergy intensity and environmental consequences of the medical face masks curtailing the COVID-19 pandemic: Malign bodyguard? *J. Clean. Prod.* **2021**, *313*, 127880. [CrossRef] [PubMed]

21. Ye, S.; Li, Y.; Huang, H.; Xu, Y.; Du, S.; Wan, F.; Xie, R.; Huang, P.; Liu, B.; Dong, T.; et al. Fast and deep disinfection for face masks recycle using vacuum ultraviolet irradiation. *J. Clean. Prod.* **2022**, *368*, 133221. [CrossRef]

22. Alcaraz, J.-P.; Le Coq, L.; Pourchez, J.; Thomas, D.; Chazelet, S.; Boudry, I.; Barbado, M.; Silvent, S.; Dessale, C.; Antoine, F.; et al. Reuse of medical face masks in domestic and community settings without sacrificing safety: Ecological and economical lessons from the COVID-19 pandemic. *Chemosphere* **2022**, *288*, 132364. [CrossRef]

23. Whyte, H.E.; Joubert, A.; Leclerc, L.; Sarry, G.; Verhoeven, P.; Le Coq, L.; Pourchez, J. Reusability of face masks: Influence of washing and comparison of performance between medical face masks and community face masks. *Environ. Technol. Innov.* **2022**, *28*, 102710. [CrossRef]

24. Neri, M.; Cuerva, E.; Levi, E.; Pujadas, P.; Müller, E.; Guardo, A. Thermal, acoustic, and fire performance characterization of textile face mask waste for use as low-cost building insulation material. *Dev. Built Environ.* **2023**, *14*, 100164. [CrossRef]

25. Miah, M.J.; Pei, J.; Kim, H.; Sharma, R.; Jang, J.G.; Ahn, J. Property assessment of an eco-friendly mortar reinforced with recycled mask fiber derived from COVID-19 single-use face masks. *J. Build. Eng.* **2023**, *66*, 105885. [CrossRef]

26. Kilmartin-Lynch, S.; Saberian, M.; Li, J.; Roychand, R.; Zhang, G. Preliminary evaluation of the feasibility of using polypropylene fibers from COVID-19 single-use face masks to improve the mechanical properties of concrete. *J. Clean. Prod.* **2021**, *296*, 126460. [CrossRef] [PubMed]

27. Koniorczyk, M.; Bednarska, D.; Masek, A.; Cichosz, S. Performance of concrete containing recycled masks used for personal protection during coronavirus pandemic. *Constr. Build. Mater.* **2022**, *324*, 126712. [CrossRef] [PubMed]

28. Al-Salem, K.; Ali, M.; Almuzaiqer, R.; Al-Suhaibani, Z.; Nuhait, A. Recycling Discarded Facemasks of COVID-19 Pandemic to New Novel Composite Thermal Insulation and Sound-Absorbing Materials. *Sustainability* **2023**, *15*, 1475. [CrossRef]

29. Neubauer, K. The Determination of Metals in Disposable, Non-Medical Face Masks by ICP-OES. *ICP-OES ICP-MS Tech. Today's Spectrosc.* **2021**, *36*, 16–23.

30. Mocé-Llivina, L.; Muniesa, M.; Pimenta-Vale, H.; Lucena, F.; Jofre, J. Survival of bacterial indicator species and bacteriophages after thermal treatment of sludge and sewage. *Appl. Environ. Microbiol.* **2003**, *69*, 1452–1456. [CrossRef] [PubMed]

31. Riddell, S.; Goldie, S.; Hill, A.; Eagles, D.; Drew, T.W. The effect of temperature on persistence of SARS-CoV-2 on common surfaces. *Virol. J.* **2020**, *17*, 145. [CrossRef]

32. Bhatia, S.; Beltramini, J.; Do, D.D. Temperature programmed analysis and its applications in catalytic systems. *Catal. Today* **1990**, *7*, 309–438. [CrossRef]

33. *UNI EN 12086:2013*; Thermal Insulating Products for Building Applications—Determination of Water Vapor Transmission Properties. UNI: Milano, Italy, 2013.

34. *UNI ISO 8301:1991*; Thermal Insulation—Determination of Steady-State Thermal Resistance and Related Properties—Heat Flow Meter Apparatus. ISO: Geneva, Switzerland, 1991.

35. *EN 1946-2:1999*; Thermal Performance of Building Products and Components—Specific Criteria for the Assessment of Laboratories Measuring Heat Transfer Properties—Part 2: Measurements by Guarded Hot Plate Method. UNI: Milano, Italy, 1999.

36. Zhang, S.; Horrocks, A.R. A review of flame retardant polypropylene fibres. *Prog. Polym. Sci.* **2003**, *28*, 1517–1538. [CrossRef]

37. Manić, N.; Janković, B.; Stojiljković, D.; Angelopoulos, P.; Radojević, M. Thermal characteristics and combustion reactivity of coronavirus face masks using TG-DTG-MS analysis. *J. Therm. Anal.* **2022**, *147*, 10131–10143. [CrossRef] [PubMed]

38. Majewsky, M.; Bitter, H.; Eiche, E.; Horn, H. Determination of microplastic polyethylene (PE) and polypropylene (PP) in environmental samples using thermal analysis (TGA-DSC). *Sci. Total Environ.* **2016**, *568*, 507–511. [CrossRef] [PubMed]

39. Seidi, F.; Movahedifar, E.; Naderi, G.; Akbari, V.; Ducos, F.; Shamsi, R.; Vahabi, H.; Saeb, M.R. Flame retardant polypropylenes: A review. *Polymers* **2020**, *12*, 1701. [CrossRef]

40. Dong, Y.; Kong, J.; Mousavi, S.; Rismanchi, B.; Yap, P.S. Wall Insulation Materials in Different Climate Zones: A Review on Challenges and Opportunities of Available Alternatives. *Thermo* **2023**, *3*, 38–65. [CrossRef]